Temperature changes of *I-V* characteristics of photovoltaic cells as a consequence of the Fermi energy level shift

Martin Libra*, Vladislav Poulek, Pavel Kouřím

Department of Physics, Faculty of Engineering, Czech University of Life Sciences Prague, Prague, Czech Republic

*Corresponding author: libra@tf.czu.cz

Abstract

Libra M., Poulek V., Kouřím P. (2017): Temperature changes of I-V characteristics of photovoltaic cells as a consequence of the Fermi energy level shift. Res. Agr. Eng., 63: 10-15.

Current voltage (*I-V*) characteristic of illuminated photovoltaic (PV) cell varies with temperature changes. The effect is explained according to the solid state theory. The higher the temperature, the lower the open-circuit voltage and the higher the short-circuit current. This behaviour is explained on the basis of band theory of the solid state physics. The increasing temperature causes a narrowing of the forbidden gap and a shift of the Fermi energy level toward the centre of the forbidden gap. Both these effects lead to a reduction of the potential barrier in the band diagram of the illuminated PN junction, and thus to a decrease of the photovoltaic voltage. In addition, narrowing of the forbidden gap causes higher generation of electron-hole pairs in the illuminated PN junction and short-circuit current increases.

Keywords: PV cell; energy band structure; PN junction; semiconductor diode; I-V characteristics

Photovoltaic (PV) energy conversion has grown in importance in the past decade. Number of large PV power plants with nominal power of the order of tens of MW_p and a number of smaller PV systems on the roofs were installed (POULEK, LIBRA 2010). Most of them were installed in Europe, mainly in connection with the subsidy policies of some countries.

It is known that changes in operation temperature cause changes of current and voltage of PV cells and PV modules (i.e. *I-V* characteristic). Increasing temperature decreases the open-circuit voltage. This effect simultaneously increases the short-circuit current (Orioli, Di Gangi 2013; Barukcic et al. 2014; Baig et al. 2015). The efficiency of the photovoltaic energy conversion thus decreases with the increasing temperature (Karatepe et al. 2007). In this paper, this phenomenon is theoretically explained by the theory of solid state physics (Pikus 1965; Snejdar, Frank 1976; Kittel 2005). Similar problems were discussed previously (Carrero et al. 2011; Liu et al. 2011; Ding

et al. 2014) in case of common solar cells or by (Strebkov 2010) in case of matrix solar cells. The *I-V* and *P-V* characteristics of partially shaded PV system were also discussed (Kofinas et al. 2015).

Nomenclature

I – electric current (A)

V – voltage (V)

 I_{x} – radiation intensity (lx)

λ – wavelength (nm)

T – temperature (K)

 \vec{E} – electric field intensity (V·m⁻¹)

E – energy (eV)

- Fermi energy (eV)

 E_{V} – top energy level of the valence band (eV)

 E_{c} – bottom energy level of the conduction band (eV)

 E_i – intrinsic number density (eV)

 E_{A} – acceptor ionisation energy (eV)

 $E_{\rm D}$ – donor ionisation energy (eV)

 $\Delta E_{\rm G}$ – energy gap (eV)

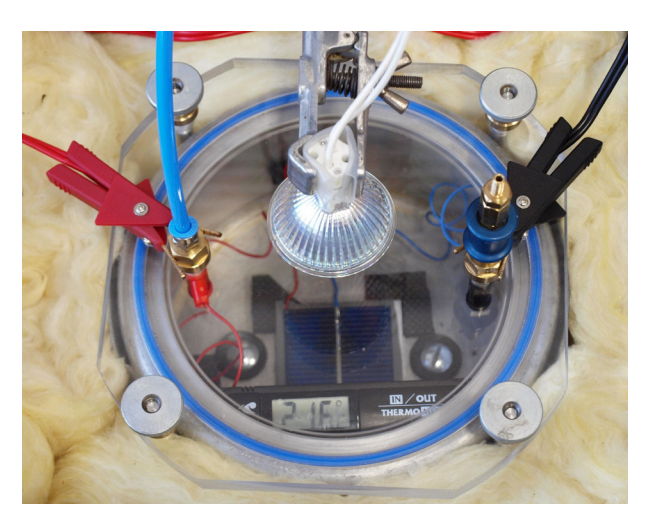


Fig. 1. Apparatus for measurement of *I-V* characteristics

 $V_{\rm p}~$ – photovoltaic voltage (V)

 $V_{\rm D}$ – diffusion voltage (V)

 e^{-} – electron charge (1.602·10⁻¹⁹ C)

 $N_{\rm A}~$ – acceptor concentration (cm $^{-3}$)

 $N_{\rm D}$ – donor concentration (cm⁻³)

h – Planck constant (6.626·10⁻³⁴ J·s)

 ν – frequency (s⁻¹)

P – power (W)

MATERIAL AND METHODS

A vacuum chamber was used to measure the *I-V* characteristics and their temperature dependence.

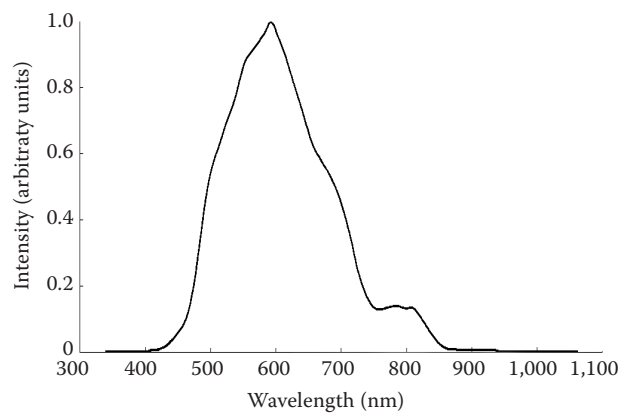


Fig. 3. Spectrum of the radiation incident on the PV cell

It was pumped by the rotary oil pump to a pressure of about 3,000 Pa. Measurements were carried out under reduced pressure so that the samples at low temperature steamed up due to atmospheric moisture. The halogen reflector lamp was used for illumination. It shined into the chamber through the window of plexiglass, irradiation intensity was measured by digital luxmeter LX 1108 (Voltcraft, Germany). Typical measurements were carried out at irradiation intensity $I_r = 35,000$ lx. The temperature was stabilized using the Peltier module and measured by a calibrated thermistor. To help stabilize the temperature the heat insulation round the vacuum chamber was used. PV cell sample was placed on an aluminium plate covered with a ther-

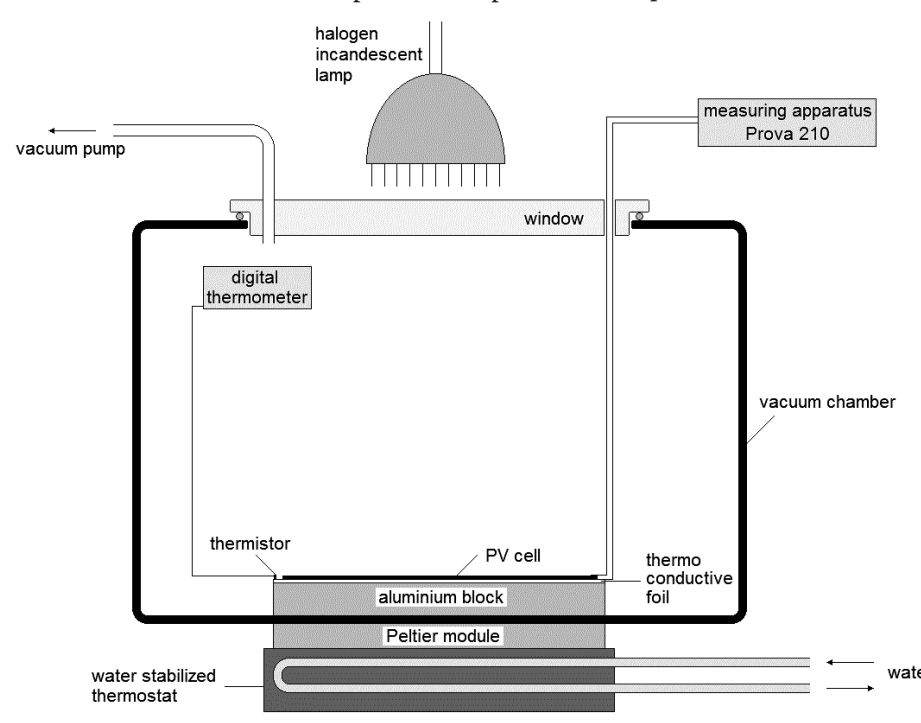


Fig. 2. Apparatus for measurement of *I-V* characteristics

Vol. 63, 2017 (1): 10–15 Res. Agr. Eng.

doi: 10.17221/38/2015-RAE

moconductive foil. Semiautomatic apparatus Prova 210 (Prova Instruments Inc., Taiwan) was used for measurement of I-V characteristics. The whole apparatus is shown in Fig. 1 and its scheme is in Fig. 2.

The spectrum of the radiation incident on the PV cell is shown in Fig. 3. Filament of the halogen lamp shines like a black body at temperature T = 3,200 K. A part of the radiation especially in the near infrared region of the spectrum is modified by infrared transparency of the reflector and by absorption in the plexiglass window. The width of the forbidden gap of silicon is approximately $E_G^{}$ = 1.1 eV at temperature T = 273 K, it decreases with the increasing temperature. Photovoltaic energy conversion can be therefore caused by photons with wavelengths shorter than $\lambda \le 1,100$ nm. These photons have sufficient energy to induce transition of an electron from the valence band into the conduction band. The irradiation intensity is low in the wavelengths region of 900 nm $\leq \lambda \leq 1{,}100$ nm, but the sensitivity of PV cells is low in this range. The highest sensitivity of crystalline PV cells is in the wavelength region of 500 nm $\leq \lambda \leq$ 900 nm (Poulek, Libra 2010) and such radiation is incident on the PV cell.

RESULTS AND DISCUSSION

Typical results of measurement of the *I-V* characteristics at different temperatures are shown in Fig. 4. It is obvious that, as expected, the individual curves intersect each other. PV cell open-circuit voltage decreases and short circuit current increases with increasing temperature. Fig. 5 shows se-

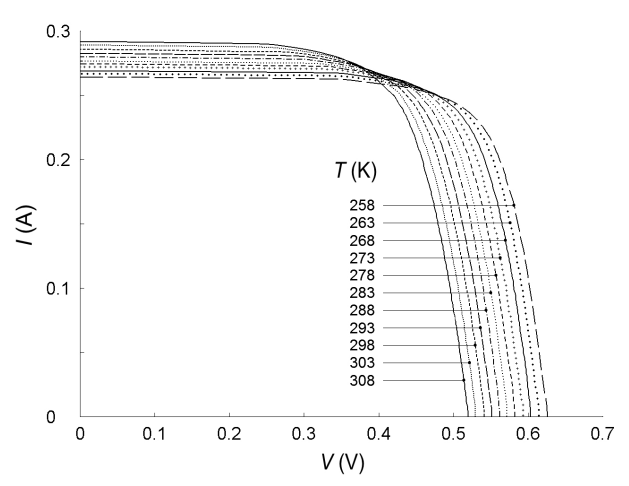


Fig. 4. Typical I-V characteristics of the PV cell at different temperatures

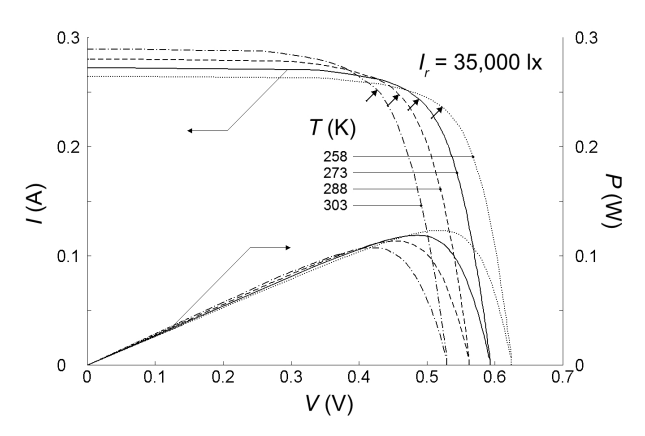


Fig. 5. Selected *I-V* characteristics with corresponding *P-V* characteristics at different temperatures

lected I-V characteristics with corresponding P-V characteristics simultaneously. The points depending on the performance and corresponding with the maximum power on the I-V characteristics are indicated by the arrow.

It can be theoretically explained by use of the band theory of solid state physics (Frank, Snejdar 1976; KITTEL 2005). This situation is illustrated schematically in Fig. 6. Fig. 6a is a diagram of the energy levels in the P-type and N-type semiconductors. Fig. 6b illustrates the equalization of the Fermi energy and bending of bands in the PN junction in a non-illuminated photovoltaic cell. Also the diffusion current and ohmic current in the equilibrium state are depicted. The regions of space charge and the diffusion voltage V_D are depicted as well. In darkness the PV cell behaves as a semiconductor diode.

Fig. 6c shows the situation after illuminating of the PV cell not connected to an electric circuit. Incident photons disturb the original equilibrium and establish a different equilibrium. Electron-hole pairs generation increases. Generated electrons and holes are accelerated in the region of the PN junction in the electric field \vec{E} in the direction of the arrows (actually in the reverse direction, corresponding to current flowing from the negative to positive pole cross the current source). The P-type side becomes charged positively and the N-type side becomes charged negatively. The potential barrier $V_{\scriptscriptstyle D}$ decreases and the Fermi levels in the P-type and N-type regions separate. The potential difference between the regions is equivalent to the photovoltaic voltage $V_{\mbox{\tiny p}^{\prime}}$ denoted in the figure. At most, this voltage could correspond to compensation of the original bending of bands, which is usually approximately $V_{\rm P} \approx 0.6~{\rm V}$ in the silicon PV

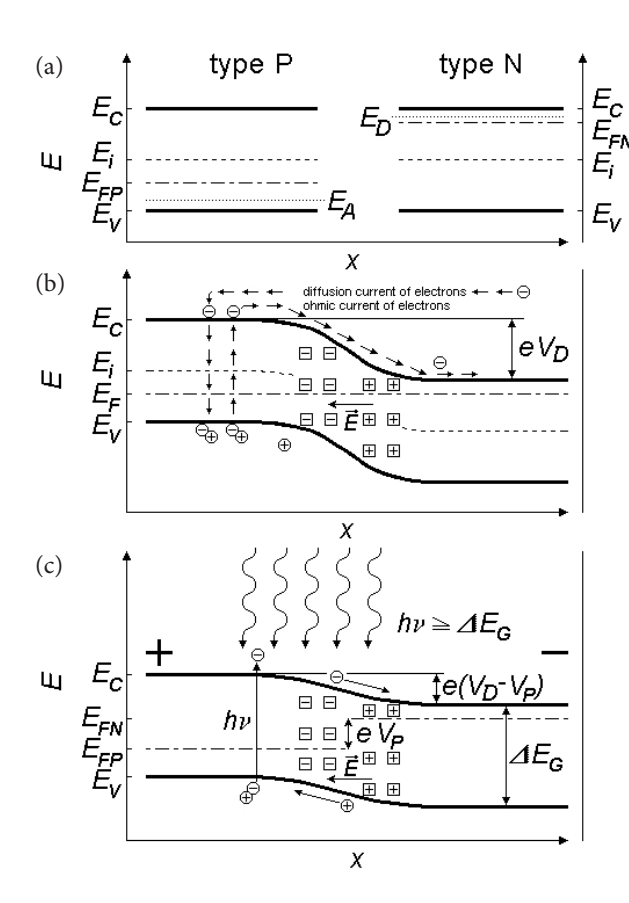


Fig. 6. Band structure of energy levels – (a) semiconductor type P, N, (b) not illuminated PN junction, and (c) illuminated PN junction

cells. The exact value depends on the doping of regions P, N and on the temperature. Further increase of the irradiation intensity does not increase the opencircuit voltage, as shown in Fig. 7. There is a limitary value of the photovoltaic open-circuit voltage. This occur since the photovoltaic potential and opposing space charge potential balance at the PN junction; further, in the PN junction, the directions of motion of generated electrons and holes movements are no longer separated. The process can also be interpreted as decreasing the potential barrier V_D by illumination results in increased diffusion current of electrons into the P-type semiconductor and increased diffusion current of holes into the N-type. This compensates for the increased ohmic current caused by the separation of the generated electrons and holes in the electric field \vec{E} between the fixed space charges in the region of the PN junction. The resulting photovoltaic voltage contributes to the establishment of a new equilibrium. The limitary value of the photovoltaic open-circuit voltage corresponds with the equalization of the original bending of the bands in the PN

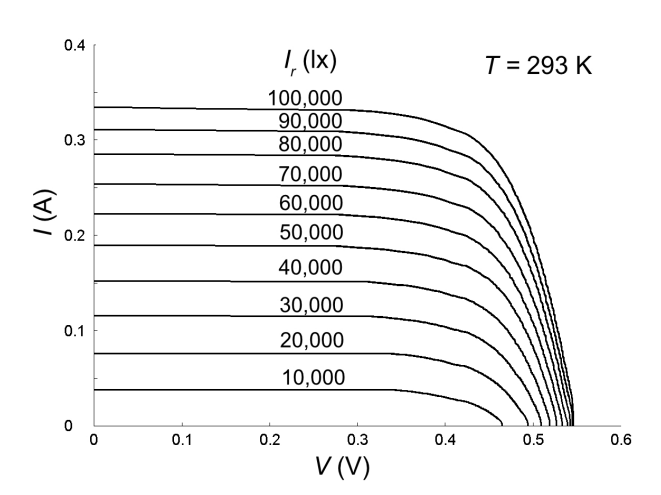


Fig. 7. Typical *I-V* characteristics of the PV cell at different irradiation intensity and constant temperature

junction; in this case, there is the maximum separation of Fermi energy levels.

If illuminated PV cell is connected into an electric circuit, the conductive connection of the two poles means reduction of photovoltaic voltage (in this case electromotive force of the source) and thus a change in the curvature of the bands leading to the repeated increase of the potential barrier $V_D - V_P$. This reduces the diffusion current and predominates ohmic current due to separation of generated electrons and holes in the electric field *E* between the fixed space charges. The sum of both currents is thus no longer zero, as it was in the case of the PV cell unconnected in the circuit. The resulting current will supply the electric circuit, the PV cell will be the source. If the resistance in the circuit decreases at a constant temperature from an infinite value to zero, then the operating point of the source moves along the curve in Fig. 5 from the open-circuit voltage to the short-circuit cur-

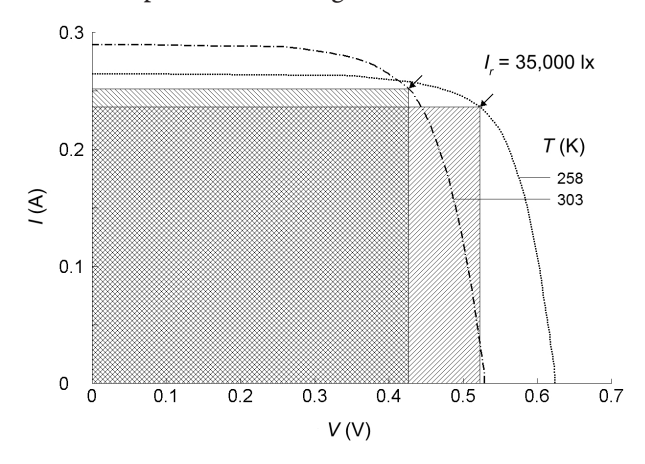


Fig. 8. Optimal operating points on I-V characteristics at two temperatures

Vol. 63, 2017 (1): 10–15 Res. Agr. Eng.

doi: 10.17221/38/2015-RAE

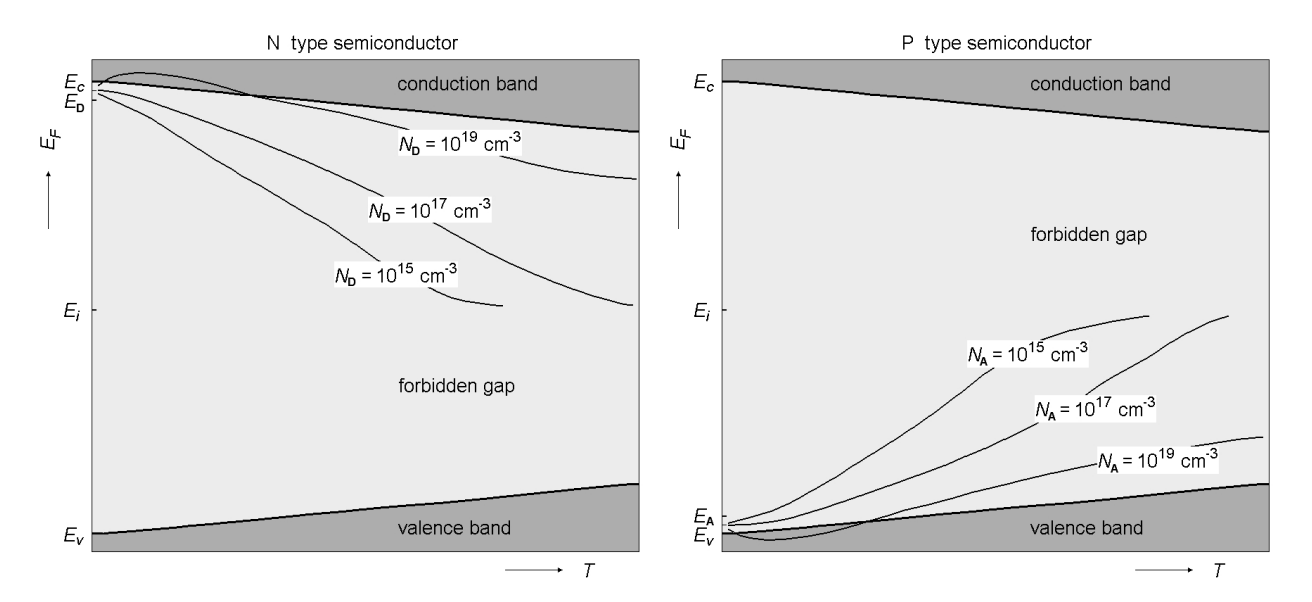


Fig. 9. Dependence of the Fermi energy level and forbidden band width (energy gap) on temperature at three dopant concentrations

rent. Optimal operating points are shown by arrows on the curves, the area of the rectangle determined by axes and by the working point is the largest; there the source provides the max. power in the electric circuit. This case is demonstrated in Fig. 8.

If the temperature increases, the Fermi energy level is shifted toward the centre of the forbidden gap and the gap narrows, as shown in Fig. 9, see also e.g. (Pikus 1965; Frank, Snejdar 1976; Hies-LMAIR 1999). It is clear from the Fig. 6c and Fig. 9, that the increasing temperature causes reduction in the photovoltaic voltage $\boldsymbol{V_p}$ at the constant irradiation intensity. Simultaneously, at higher temperature of the forbidden gap in the band structure of energy levels is narrower. It affects a higher generation of electron-hole pairs in the illuminated PN junction and increase of the ohmic current. Decrease of the maximum power supply by the PV cell corresponds with the maximum area of the abovementioned rectangle, as shown in Fig. 8. Thus, with increasing temperature of PV cells the efficiency of photovoltaic energy conversion also decreases. If the temperature approaches approximately 500 K, the conversion efficiency approaches to zero.

CONCLUSION

Behaviour of the temperature dependences of *I-V* characteristics of illuminated PV cells was theoretically explained on the basis of band theory of solid

state physics. The temperature increase causes a shift of the Fermi energy level toward the centre of the forbidden gap and the gap narrowing. It leads to reduction of the potential barrier in the band diagram of the PN junction and to reduction of the photovoltaic voltage V_p . Simultaneously, the higher temperature causes narrowing of the forbidden gap in the band structure of energy levels. It affects a higher generation of electron-hole pairs in the illuminated PN junction and increases of the ohmic current. The efficiency of the photovoltaic energy conversion decreases with increasing temperature. These effects are illustrated in the diagram of the band structure of energy levels of the PN junction.

It should be emphasized that the experimental cells were cut near the bus bar so the influence of the temperature-dependent ohmic loss of the current collection grid can be neglected. This effect could be significant especially in the case of radiation concentration for example by total internal reflection reported likewise in (BAIG et al. 2015) or by Fresnel lens reported in (Chemisana 2011).

References

Baig H., Sellami N., Mallick T.K. (2015): Performance modeling and testing of a Building Integrated Concentrating Photovoltaic (BICPV) system. Solar Energy Materials & Solar Cells, 134: 29–44.

Barukcic M., Hederic Z., Spoljaric Z. (2014): The estimation of *I–V* curves of PV panel using manufacturers' *I–V*

- curves and evolutionary strategy. Energy Conversion and Management, 88: 447–458.
- Carrero C., Ramírez D., Rodríguez J., Platero C.A. (2011): Accurate and fast convergence method for parameter estimation of PV generators based on three main points of the *I-V* curve. Renewable Energy, 36: 2972–2977.
- Ding K., Zhang J., Bian X., Xu J. (2014): A simplified model for photovoltaic modules based on improved translation equations. Solar Energy, 101: 40–52.
- Frank H., Snejdar V. (1976): Principy a vlastnosti polovodičových součástek. Prague, SNTL.
- Hieslmair H., Istratov A.A., Flink C., McHugo S.A., Weber E.R. (1999): Experiments and computer simulations of iron profiles in p/p⁺ silicon: segregation and the position of the iron donor level. Physica B, 273–274: 441–444.
- Chemisana D., Ibanez M., Rosell J.I. (2011): Characterization of a photovoltaic-thermal module for Fresnel linear concentrator. Energy Conversion and Management, 52: 3234–3240.
- Karatepe E., Boztepe M., Colak M. (2007): Development of a suitable model for characterizing photovoltaic arrays with shaded solar cells. Solar Energy, 81: 977–992.

- Kittel Ch. (2005): Introduction to Solid State Physics. John Wiley & Sons, Inc.
- Kofinas P., Dounis A.I., Papadakis G., Assimakopoulos M.N. (2015): An Intelligent MPPT controller based on direct neural control for partially shaded PV system. Energy and Buildings, 90: 51–64.
- Liu G., Nguang S.K., Partridge A. (2011): A general modeling method for *I–V* characteristics of geometrically and electrically configured photovoltaic arrays. Energy Conversion and Management, 52: 3439–3445.
- Orioli A., Di Gangi A. (2013): A procedure to calculate the five-parameter model of crystalline silicon photovoltaic modules on the basis of the tabular performance data. Applied Energy, 102: 1160–1177.
- Pikus G.E. (1965): Basic theory of semiconductor devices. Moscow, Nauka.
- Poulek V., Libra M. (2010): Photovoltaics. Prague, ILSA. Strebkov D.S. (2010): Матричные солнечные элементы, Moscow, ВИЭСХ.

Received for publication April 21, 2015 Accepted afeter corrections March 15, 2016